Controlled synthesis and structure tunability of photocatalytically active mesoporous metal-based stannate nanostructures

Caihong Liu [a], Haiyan Chen [b], Zheng Ren [a], Sameh Dardona [c], Martin Piech [c], Haiyong Gao [a], Pu-Xian Gao [a,*]

[a] *Department of Materials Science and Engineering & Institute of Materials Science, University of Connecticut, Storrs, CT 06269-3136, United States*
[b] *Mineral Physics Institute, Stony Brook University, Stony Brook, NY 11794, United States*
[c] *Department of Physical Sciences, United Technologies Research Center, East Hartford, CT 06108, United States*

ARTICLE INFO

ABSTRACT

A variety of stannate nanostructures have been fabricated for UV photocatalysis, including zinc- and cadmium-based stannates. As the template nanostructures, high surface-area mesoporous metal hydroxystannate [$ZnSn(OH)_6$ and $CdSn(OH)_6$] nanoparticles (>$100\,m^2$/g) have been synthesized using a simple, low-temperature substitution chemical process with controlled porosity, morphology and crystallinity. Post-synthetic thermal treatments were employed to obtain amorphous $ZnSnO_3$, $CdSnO_3$, ilmenite $CdSnO_3$, and crystalline Zn_2SnO_4–SnO_2 nanoparticles. As a result, the band gaps can be tuned from 5.4 eV to 3.3 eV and from 4.9 eV to 2.1 eV for Zn-based and Cd-based stannates, respectively. Amorphous $ZnSnO_3$ porous nanoparticles showed highest activity toward dye degradation under UV illumination followed by the Zn_2SnO_4-SnO_2 and ilmenite $CdSnO_3$ nanostructures due to their beneficial band structure alignment, high conductivities, and high specific surface areas. This study may provide an important strategy for high throughput synthesis and screening of functional complex metal oxide nanomaterials, while the enabled stannate nanomaterials could be utilized in various applications.

© 2014 Elsevier B.V. All rights reserved.

1. Introduction

Ternary metal oxides incorporating two types of multi-valence metal cations and typically including ABO_3 and A_2BO_4 constitute an important category of functional materials with applications in electronics and communication areas due to their unique optical, electronic, and magnetic properties [1–4]. The co-existence of two different metal ions within ternary metal oxide structures requires a robust stoichiometry control during the synthesis. Moreover, the high material purity required in some applications asks for the fine-tuning of synthesis procedures, as well as the design of differentpost-synthetic treatments. The ability to rationally modulate composition in ternary compound nanomaterials would allow the structure and property tunability, thus offering a new class of versatile building blocks for nanoscale electronics and photonics. However, to date, a limited number of studies [5–7] have been reported on the structure and property modulation within ternary metal oxide systems.

Recently, tin-based ternary oxide (stannate) materials have attracted considerable attention due to their versatile applicability

and large material family. The typical stannates include perovskite-type metal hydroxystannate [$MSn(OH)_6$], metal stannate [$MSnO_3$], and di-metal stannate [M_2SnO_4] characterized by a spinel cubic crystal structure. For example, Zinc-based stannate materials are important for energy and environment related applications including flame retardant and smoke suppressant [8,9], photoelectrochemical cells [10–12], transparent conductive electrodes [13,14], Li-ion batteries [15], photocatalysts [16,17], and sensors [18–21]. Similarly, Cadmium-based stannate nanomaterials including $CdSnO_3\cdot3H_2O$, $CdSnO_3$, Cd_2SnO_4 have also been demonstrated in gas sensing [22,23], solar energy utilization [24–26], Li-ion battery [27], and transparent conducting electrodes [28]. With similar applications and similar composition and properties, comparative and detailed studies are needed to further understand the relationship of composition, structure and property in these stannate nanomaterials. This can benefit the material design and screening for various functional applications.

In this work, a simple, generic and low temperature substitution reaction in aqueous solution has been utilized to synthesize various mesoporous perovskite hydroxystannate ($MSnO_3\cdot3H_2O$ or $MSn(OH)_6$, M = Zn, Cd) nanoparticles. These structures were subsequently used as template for various Zn/Cd-based stannate nanoparticles through different post-synthetic annealing treatments. Their structure evolutions after thermal treatments were

characterized using multiple characterization tools such as electron microscopies and spectroscopies, through which morphology, composition, and polymorph evolutions were identified. More stannates were identified, including porous ZnSnO₃ (ZS) and Zn₂SnO₄ (DZS) for Zn-based stannate and amorphous CdSnO₃ (a-CS) and ilmenite CdSnO₃ (c-CS) for Cd-based stannate. Their optical-electronic structure and photocatalytic properties were investigated. Among them, amorphous ZS porous nanoparticles showed the highest activity toward dye degradation under UV illumination, followed by DZS-SnO₂ and ilmenite CdSnO₃ nanostructures. It is suggested that favorable band alignment, high carrier mobility, and large specific surface area are key features for highly efficient photocatlysts.

2. Experiments

2.1. Materials preparation

ZnSn(OH)₆ (zinc hydoxystannate, ZHS) & CdSn(OH)₆ (cadmium hydroxystannate, CHS) nanoparticles were hydrothermally synthesized based on the following reaction:

$$MSO_4 + Na_2SnO_3 \cdot 3H_2O \rightarrow MSnO_3 \cdot 3H_2O \downarrow + Na_2SO_4 \, (M = Zn, \, Cd). (1)$$
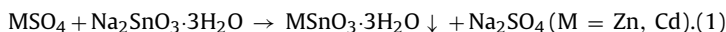
All reagents were of analytical grade and used without further purification. Equal mole and concentration (10 mM) of ZnSO₄·6H₂O or CdSO₄·3/8H₂O (for synthesis of ZHS or CHS) and Na₂SnO₃·3H₂O aqueous solutions were prepared separately at room temperature until reagents dissolved completely in deionized water. Subsequently, the Na₂SnO₃ was added dropwise to ZnSO₄ or CdSO₄ aqueous solution while vigorously stirring at 0 °C, room temperature or 60 °C. After that, the reaction mixture was kept stirring for 12 h under the same temperature. The resultant precipitates were collected by microfiltration, rinsed several times with deionized water, and dried for 12 h in 80 °C oven.

2.2. Materials characterization

Crystal structure and composition of the obtained samples were investigated by X-ray diffraction (XRD). The XRD was conducted at room temperature using a Bruker AXS D8 ADVANCE diffractometer (Cu Kα radiation, λ = 1.541 Å) with the accelerating voltage, emission current, and scanning speed of 40 kV, 40 mA, and 5°/min, respectively. The specific surface areas and pore size distributions were determined by Brunauer–Emmett–Teller (BET) nitrogen adsorption and desorption method via a Micromeritics ASAP 2020 physi-sorption analyzer. Before the measurement, the samples were degassed at 120 °C (for ZHS and CHS) or 360 °C (for the products after thermal decomposition, such as ZS, CS, etc.) for 8 h. The pore size distributions were calculated using the Barret–Joyner–Halenda (BJH) model based on nitrogen desorption isotherms. The composition, structure and morphology of ZHS/CHS and their derived stannate nanoparticles were characterized using scanning electron microscopes (SEM) (JEOL 6335F FE-SEM and FEI Quanta SEM), scanning transmission electron microscope (STEM, Philips Tecnai-12 STEM, 120 kV) both equipped with energy dispersive X-ray spectrometers (EDXS). A JEOL 2010 High resolution TEM (accelerating voltage: 200 kV) was used to acquire atomistic lattice images of various stannate nanostructures. Based on the microscopic images, about 300 nanoparticles were considered for each sample to obtain their size distribution histograms. Thermogravimetric analysis (TGA) and differential scanning calorimeter (DSC) were carried out using the TA Instruments Q600 in a nitrogen atmosphere with ceramic sample pans. The data were collected with a scan rate of 5 °C/min over a temperature range of 0–1000 °C. The stannate thin films were fabricated via the following procedure for film absorption spectra and film conductivity test: first, ZHS/CHS paste was prepared by dispersing ZHS/CHS nanoparticles (0.3 g) powder and Triton X-100 (0.02 g) in water (2 mL) containing some acetylacetone (~0.8 mL); then the paste was spread uniformly on the surface of the quartz using the doctor-blade technique with adhesive tape (Scotch brand) as frame and spacer, followed by heating in air at 80 °C for several hours to remove solvents. Further thermal annealing was applied to get amorphous ZS or CS (350 °C, 9 h), DZS-SnO₂ or ilmenite CS (850 °C, 9 h) films, as well as to remove surfactant. The ZHS/CHS film for conductivity test was just fabricated by drop-cast their isopropanol suspension on quartz to form a continuous film. No surfactant was added. Afterwards, Varian Cary 5000 and Perkin Elmer ultraviolet–visible–near infrared (UV–Vis-NIR) spectrophotometer were used for optical absorption measurements. Film surface resistivities were tested using Keithley 4200 SCS analyzer combined with 4-point linear probe head (Signatone Co., model: SP4). Commercial FTO (~13 Ω/sq.) and ITO (~100 Ω/sq.) glass are used to test the reliability of the above system.

2.3. Photocatalytic studies

In a typical experiment, stannate nanoparticles (20 mg) were dispersed in a 50 mL vial containing 20 mL ~5 mg/L of aqueous Rhodamine B (RB). Prior to irradiation, the mixture was sonicated in darkness for 15–30 min to establish the adsorption/desorption equilibrium. The suspensions were then centrifuged. The UV-Vis spectrum of the supernatant was taken to determine the initial concentration of the RB solution before photocatalysis test (C_0). Afterward, the suspension was irradiated with a 22 W UV lamp (Luzchem, USA, 5.9 mW/cm²) having emission peak centered at 350 nm. A 150-W solar simulator (Model: 96000, Newport optics) with an Air mass 1.5 global filter was used as a general light source (beam diameter: 5 cm). The above light beam was passed through bandpass filters (λ = 300 and 420 nm, band width ~10 nm, beam diameter: 2.5 cm) to generate monochromatic UV lights. A dual-band Handheld UV Lamp (UVP LLC., Model: UVGL-55) was employed for 254 nm and 365 nm mono-UV lights. The monochromatic light intensity was measured by an optical power meter (Model: 842-PE, Newport optics) combined with a thermopile sensor (Model: 818P-040-25, Newport optics). Distance between the lamp and samples are controlled so that the beam power density of these monochromatic lights illuminated on samples are identical, i.e., ~1 mW cm⁻².

Degradation was monitored by analyzing aliquots withdrawn from the suspension at various irradiation time intervals. The aliquot samples containing the photocatalyst and RB were centrifuged, and the absorption spectra of the supernatant solutions were recorded in the 400–700 nm spectral range. The RB concentrations were determined using the Beer–Lambert law $A = \alpha c \ell$, where A is the maximum RB absorbance around 557 nm, α is the RB molar absorptivity, and ℓ is the sample cell length (1 cm). RB degradation was expressed as C/C_0 versus UV-irradiation time.

3. Results and discussion

A low-cost, green, and generic synthetic method was used to synthesize ZnSn(OH)₆ [29] and CdSn(OH)₆ nanoparticles with controlled size and morphology. Simply by mixing M^{n+} (such as Zn²⁺ or Cd²⁺) solution with Na₂SnO₃·3H₂O aqueous solution, a variety of perovskite metal hydroxystannate nanoparticles were obtained. Their typical TEM and SEM images were illustrated in Figs. 1 and S1. The reaction temperature and precursor concentrations were found to play important roles in tuning the size, morphology, and crystallinity of the ZHS and CHS nanoparticles. When the reaction processed at 0 °C, polycrystalline perovskite ZHS